

The ICESat-2 Laser Altimetry Mission

Planned to launch in 2015, ICESat-2 will measure changes in polar ice coverage and estimate changes in the Earth's bio-mass by measuring vegetation canopy height.

By WALEED ABDALATI, H. JAY ZWALLY, ROBERT BINDSCHADLER, BEA CSATHO, SINEAD LOUISE FARRELL, HELEN AMANDA FRICKER, DAVID HARDING, RONALD KWOK, MICHAEL LEFSKY, THORSTEN MARKUS, ALEXANDER MARSHAK, THOMAS NEUMANN, STEPHEN PALM, BOB SCHUTZ, BEN SMITH, JAMES SPINHIRNE, AND CHARLES WEBB

ABSTRACT | Satellite and aircraft observations have revealed that remarkable changes in the Earth's polar ice cover have occurred in the last decade. The impacts of these changes, which include dramatic ice loss from ice sheets and rapid declines in Arctic sea ice, could be quite large in terms of sea level rise and global climate. NASA's Ice, Cloud and Land Elevation Satellite-2 (ICESat-2), currently planned for launch in 2015, is specifically intended to quantify the amount of change in ice sheets and sea ice and provide key insights into their

behavior. It will achieve these objectives through the use of precise laser measurements of surface elevation, building on the groundbreaking capabilities of its predecessor, the Ice Cloud and Land Elevation Satellite (ICESat). In particular, ICESat-2 will measure the temporal and spatial character of ice sheet elevation change to enable assessment of ice sheet mass balance and examination of the underlying mechanisms that control it. The precision of ICESat-2's elevation measurement will also allow for accurate measurements of sea ice freeboard height, from which sea ice thickness and its temporal changes can be estimated. ICESat-2 will provide important information on other components of the Earth System as well, most notably large-scale vegetation biomass estimates through the measurement of vegetation canopy height. When combined with the original ICESat observations, ICESat-2 will provide ice change measurements across more than a 15-year time span. Its significantly improved laser system will also provide observations with much greater spatial resolution, temporal resolution, and accuracy than has ever been possible before.

Manuscript received May 29, 2009; revised September 23, 2009. Current version published May 5, 2010. This work was supported by the ICESat-2 Program, NASA, and the Cryospheric Sciences Program, NASA.

W. Abdalati is with the Earth Science and Observation Center and Department of Geography, University of Colorado at Boulder, Boulder, CO 80302 USA (e-mail: waleed.abdalati@colorado.edu).

H. J. Zwally, R. Bindshadler, D. Harding, T. Markus, A. Marshak, and T. Neumann are with the Science and Exploration Directorate, NASA Goddard Space Flight Center, Greenbelt, MD 20771 USA (e-mail: zwally@icesat2.gsfc.nasa.gov; robert.a.bindshadler@nasa.gov; David.J.Harding@nasa.gov; thorsten.markus-1@nasa.gov; alexander.marshak-1@nasa.gov; thomas.neumann@nasa.gov).

B. Csatho is with the Department of Geology, University at Buffalo, Buffalo, NY 14260 USA (e-mail: bcsatho@buffalo.edu).

S. L. Farrell is with the Cooperative Institute for Climate Studies, University of Maryland, College Park, MD 20742 USA (e-mail: Sinead.Farrell@noaa.gov).

H. A. Fricker is with the Scripps Institution of Oceanography, San Diego, CA 92121 USA (e-mail: hafriicker@ucsd.edu).

R. Kwok is with the Jet Propulsion Laboratory, California Institute of Technology, 91125 USA (e-mail: ronald.kwok@jpl.nasa.gov).

M. Lefsky is with Colorado State University, Fort Collins, Colorado 80125 USA (e-mail: lefsky@gmail.com).

S. Palm is with Science Systems and Applications Inc., Lanham, MD 20706 USA (e-mail: Stephen.P.Palm@nasa.gov).

B. Schutz and C. Webb are with the Center for Space Research, University of Texas at Austin, 78712 USA (e-mail: schutz@csr.utexas.edu; cwebb@mail.utexas.edu).

B. Smith is with the Polar Science Center, University of Washington, Seattle, WA 98195 USA (e-mail: bsmith@apl.washington.edu).

J. Spinirne is with the University of Arizona, Tucson, AZ 85721 USA (e-mail: jspin@email.arizona.edu).

KEYWORDS | Ice sheets; ICESat-2; laser altimetry; NASA; satellite; sea ice; vegetation

I. INTRODUCTION

Observations from satellites and aircraft have revealed that in the last decade, the Earth's polar cryosphere has experienced some remarkable changes. The Greenland and Antarctic ice sheets are losing mass at an increasing rate [1]–[3]. Fast flowing outlet glaciers and ice streams, which carry most of the mass flux from the interiors of the vast Greenland and Antarctic ice sheets toward the ocean, have

accelerated dramatically [4]–[7]. The sea ice that covers the Arctic Ocean has decreased in areal extent far more rapidly than climate models have predicted [8] and has thinned substantially [9], suggesting that a summertime ice-free Arctic ocean may be imminent. Some of the thick and ancient ice shelves that fringe the Antarctic Peninsula have disintegrated, triggering the acceleration of the outlet glaciers that feed them [10], [11]. These and other phenomena suggest that the state of balance of the Earth's polar ice cover is in transition, with much of it in a substantial negative downturn. Amidst these dramatic losses, however, some areas have experienced modest ice growth. Parts of the Greenland and Antarctic ice sheets have thickened [12]–[14], and on the whole, the Antarctic sea ice area has increased slightly in the last three decades [15]. All of these occurrences—rapid losses, slight gains, dramatic increases in ice discharge, etc.—are indicative of the dynamic complexity of polar ice.

Though far-removed from the everyday lives of most of the world's population, the behavior of ice sheets and sea ice is of major and direct consequence to society. The Greenland and Antarctic ice sheets contain enough ice to raise sea level by about 7 and 60 m, respectively [2]. Sea ice exhibits a major influence on the Earth's planetary energy budget, influencing global weather and climate; and the Arctic ice cover is especially sensitive to and a strong driver of climate change, in large part due to the positive albedo feedbacks associated with melting ice. Consequently, the Earth's polar ice cover is a critical and potentially unstable component of the Earth system. NASA's Ice Cloud and Land Elevation Satellite-2 (ICESat-2) is specifically intended to quantify the rate of change of ice sheets and sea ice and provide key insights into the processes that drive those changes. It will achieve these objectives through the use of precise laser measurements of surface elevation, following the pioneering—though compromised—capabilities demonstrated by its predecessor, the Ice Cloud and Land Elevation Satellite (ICESat). These laser altimeter measurements will also provide important information on other components of the Earth system, in particular, vegetation biomass through the measurement of vegetation canopy height.

II. BACKGROUND

On January 12, 2003, NASA launched ICESat (Fig. 1), the first satellite mission specifically designed to measure changes of polar ice, as part of NASA's Earth Observing System. ICESat combined state-of-the-art laser ranging capabilities with precise orbit and attitude control and knowledge to provide very accurate measurements of ice sheet topography and elevation change at high along-track spatial resolution. ICESat achieved this by sampling over ~ 65 -m-diameter footprints every ~ 172 m, and has elevation retrieval precision and accuracy of ~ 2 and ~ 14 cm per shot, respectively [16]. By observing changes

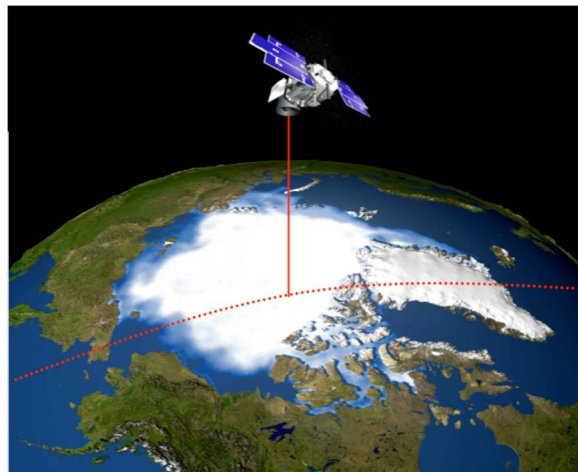


Fig. 1. Schematic diagram of ICESat on a transect over the Arctic. ICESat uses a 1064 nm laser operating at 40 Hz to make measurements at 172-m intervals over ice, oceans, and land.

in ice sheet elevation (dh/dt), it is possible to quantify the growth and shrinkage of parts of the ice sheets with great spatial detail, thus enabling an assessment of ice sheet mass balance and contributions to sea level. Moreover, because the mechanisms that control ice sheet mass loss and gain—changes in accumulation, surface ablation, and discharge—presumably have distinct topographic expressions, ice sheet elevation changes also provide important insights into the processes causing the observed changes.

The original ICESat mission's primary instrument is the Geoscience Laser Altimeter (GLAS), which carries three 1064 nm Nd-YAG lasers, each of which was expected to operate continuously for approximately 18 months to enable a nearly five-year mission [17]. GLAS also includes a frequency-doubler in the beam path that converted a portion of the main 1064 nm beam to 532 nm in order to enable more accurate atmospheric measurements, since detectors at green wavelengths are more sensitive than those in the near infrared (IR). On-orbit anomalies resulted in the premature failure of the first laser after 37 days of operation and rapid energy decay in the second laser. In the face of compromised laser life, ICESat operations were switched in fall 2003 from continuous measurement to a campaign mode, in which elevation measurements were made along repeat ground tracks for three 33-day periods (a subcycle of the more densely spaced 91-day exact repeat orbit) each year during northern hemisphere (NH) fall, winter, and spring seasons (Table 1). This revised strategy was intended to enable the mission to meet its overall ice sheet change detection objectives but with less temporal and spatial detail than would have been achieved with continuous operation. Later, beginning in 2007, the NH winter campaigns were

Table 1 Acquisition Dates and Release Numbers for the 13 91-Day ICESat Campaigns Acquired Up to March 2008

Campaign Period	Date	Millions of Shots
Laser 2a	10/04/03-11/19/03	159
Laser 2b	02/17/04-03/21/04	114
Laser 2c	05/18/04-06/21/04	118
Laser 3a	10/03/04-11/08/04	124
Laser 3b	02/17/05-03/24/05	121
Laser 3c	05/20/05-06/23/05	118
Laser 3d	10/21/05-11/24/05	118
Laser 3e	02/22/06-03/28/06	118
Laser 3f	05/24/06-06/26/06	114
Laser 3g	10/25/06-11/27/06	114
Laser 3h	03/12/07-04/14/07	114
Laser 3i	10/02/07-11/05/07	118
Laser 3j	02/17/08-03/21/08	114
Laser 3k*	10/04/08-10/19/08	38
Laser 2d*	11/25/08-12/17/08	76
Laser 2e	03/09/09-04/11/09	114
Laser 2f	09/30/09-10/11/09	33

*Laser 3 expired 10 days into the October/November 2008 campaign. The campaign was completed using the low-energy Laser 2. Diagnosing the Laser-3 failure mode and implementing the switch back to Laser 2 took about 1 month. Laser 2 expired on October 11, 2009.

dropped to further extend mission life (Table 1). The revised operations plan and the excellent performance of ICESat's third laser have enabled a total of 15 33-day measurement campaigns over a period of 5.5 years. The ICESat mission is no longer collecting elevation data as the final GLAS laser ceased firing in October 11, 2009.

Despite its compromised operation, ICESat has demonstrated a remarkable capability not only to assess changes in ice sheet elevations (e.g., [14], [18], [19], as shown in Fig. 2, but also to measure sea ice freeboard, from which thickness can be inferred [9], [20]–[23]. It has also been used to determine vegetation height and aboveground biomass [24]–[30], and for various other applications across a wide range of disciplines. In addition, ICESat has provided new insights into Antarctic subglacial hydrology through its unanticipated capability to detect localized surface deformation (subsidence or uplift) in response to movement of subglacial water beneath up to 4 km of ice [31]–[33].

It was these demonstrated capabilities, coupled with recent observations of dramatic changes in polar ice,

that led the National Research Council's Earth Science Decadal Survey to call for an ICESat follow-on mission [34]. ICESat-2 is intended to carry out the measurements that were successfully begun by ICESat despite its compromised operating condition. Advances in laser technology since the design and launch of ICESat are such that the problems experienced with ICESat's analog pulse laser system can readily be addressed with more reliable laser diodes and more benign operating conditions. In addition, developments in micropulse laser technology allow consideration of new low-energy high-repetition-rate systems to further improve the capabilities of ICESat-2.

III. ICESat-2 MISSION OBJECTIVES

Like ICESat, ICESat-2 is expected to support multidisciplinary applications; however, following from the Decadal Survey's recommendation, the main science goals are specifically targeted at measuring 1) ice sheet changes, 2) sea ice thickness, and 3) vegetation biomass. The ICESat-2

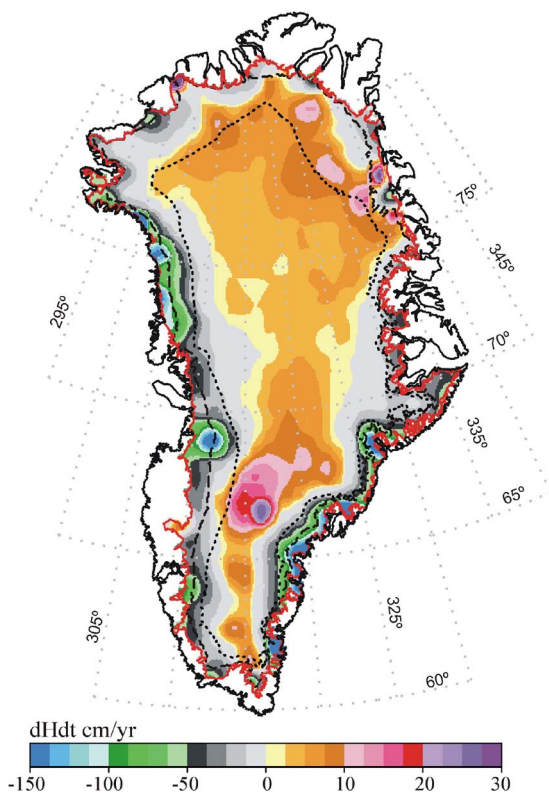


Fig. 2. Changes in ice elevation derived from ICESat repeat-track analyses for the period October, 2003 through October, 2007. The ice sheet continues to increase in elevation inland, as it did in the 1990s, but thinning at the margins has increased significantly, due to increased summer melting and acceleration of outlet glaciers. The dotted line shows the 2000-m contour line, and the dashed line shows the ice sheet equilibrium line.

Science Definition Team (SDT) has defined specific science objectives for the mission in each of these areas.

A. Ice Sheets

The primary objective of ICESat-2 is to quantify polar ice sheet contributions to sea-level rise and the linkages to climate conditions. ICESat-2 will accomplish this by measuring changes in ice sheet elevation for the purposes of assessing overall ice sheet mass balance and its variation in time and space in the context of a changing climate. Understanding the causes of that spatial and temporal variability is the key to achieving the ultimate goal of developing predictive models that will reliably estimate future ice sheet contributions to sea level.

To meet these objectives, ICESat-2 must measure elevation changes with an accuracy and resolution sufficient to isolate surface-driven change (controlled by accumulation and surface ablation variability) from dynamic imbalances (caused by accelerating or decelerating ice flow). We assume that each of these processes has a spatially variable dh/dt signature. Melt-driven imbalances, which are often under a

meter in height, should lower or raise surfaces in a manner that varies slowly over large distances, decreasing from a maximum at the margin to zero at the equilibrium line altitude [35]. Also, since surface melt is driven by atmospheric processes, it should not be significantly different between adjacent areas of fast-moving ice streams and the slow-moving ice sheet. Dynamic imbalances, which can be many meters in magnitude, begin and are usually most extreme near outlet glacier termini, propagate inward with time, and vary significantly over small scales in transition regions between ice stream flow and sheet flow [36]. Accumulation and precipitation will presumably have variable gradients that would most likely be strongest in the high accumulation zones near the margins and lowest at the low accumulation regions at the interior, and will affect elevation change both above and below the equilibrium line.

Quantifying these distinctions is very important for the development of predictive models that capture both dynamic and surface processes. Doing so requires detection of vertical changes at a level that is significantly smaller than the seasonal amplitude. It also requires the characterization of change along linear distances at major ice boundaries, such as the transition regions from slow sheet flow to fast stream flow or from grounded ice to floating ice (Fig. 3). These transition areas exhibit a strong influence on the evolution of flow. In view of these considerations, the SDT determined that ICESat-2 must be capable of resolution of winter/summer elevation change

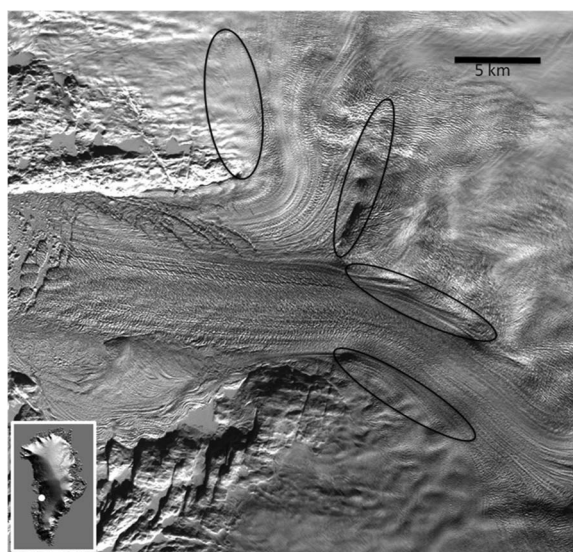


Fig. 3. Landsat image of the Jakobshavn Ice Stream from 2002. Black ovals show transition regions from sheet flow to stream flow. In these areas, knowledge of topographic change along linear transects is critical for understanding the controls of these transition zones on ice stream flow. Inset: ICESat-derived digital elevation model of Greenland (Dimarzio et al., 2007). The white dot indicates the location of the larger image.

to 2.5 cm at subdrainage basin scales ($25 \times 25 \text{ km}^2$), annually resolved elevation changes of 25 cm/y on outlet glaciers (100 km^2 areas), and annually resolved elevation changes of 25 cm/y at outlet glacier margins (along linear distances of 1 km).

B. Sea Ice

There is currently no means of directly measuring sea ice thickness by satellite; however, a useful proxy is to measure the freeboard height (the height of the surface above open water) and estimate the ice thickness based on the density differences between the floating ice, snow, and water (Fig. 4). This has been demonstrated with ERS-1, ERS-2, and Envisat radar altimetry [37], [38], and with improved spatial sampling and coverage using ICESat laser altimetry [9], [20]). Arctic Ocean sea ice thickness from two ICESat campaigns are shown in Fig. 5. Achieving this capability requires very dense and precise along-track sampling to measure the differences in height between the ice surface and that of narrow leads directly.

Unlike ice sheet elevation change, the primary measurement driver for sea ice is precision (i.e., consistency of retrievals between adjacent pulses) rather than accuracy. Because estimating thickness requires scaling the freeboard measurement by approximately a factor of ten, small errors in precision can translate to large errors in sea ice thickness. Furthermore, as snow loading depresses the sea ice freeboard, it has to be accounted for in the calculation of ice thickness. Various approaches to estimate snow depth—including the use of a snow climatology [37], snowfall from meteorological fields [9],

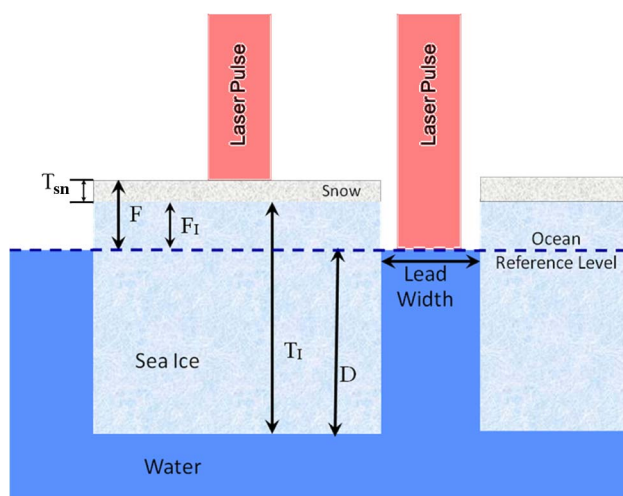


Fig. 4. Schematic diagram of sea ice showing the relationships between sea ice thickness (T_I), ice draft (D), ice freeboard (F_I), total freeboard (F), and snow thickness (T_{sn}). The laser measures to the top of the ice/snow surface, and freeboard height is determined from the difference between the reference ocean level (height within a lead) and the elevation of the ice/snow surface.

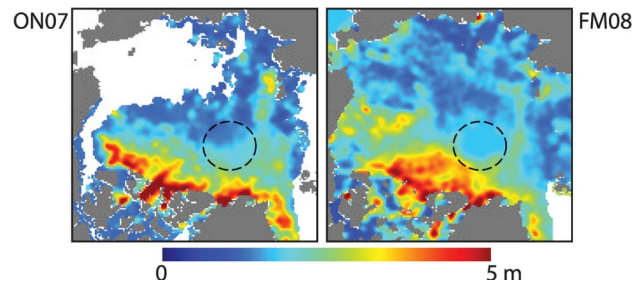


Fig. 5. Sea ice thickness for fall 2007 (ON2007) and spring 2008 (FM08) estimated from ICESat-derived freeboard height with the pole-hole filled in by interpolation and smoothed with a 50-km Gaussian kernel (Kwok et al., 2009).

and derived snow fields from passive microwave data [22]—have been used. A recent assessment [9] shows that the ICESat thickness estimates are within 0.5 m of ice thickness estimated from draft measurements from profiling sonars on submarines and ocean moorings.

Three centimeter precision (in freeboard) is a minimum required capability, which corresponds to an accuracy of $\sim 0.3 \text{ m}$ in thickness or an overall uncertainty of better than 25% of the current annual ice-volume production of the Arctic Ocean. Measurement at this level will enable accurate determination of the spatial ranges of ice thickness across the Arctic (3–4 m) and Southern (2–3 m) Oceans. It will also resolve the seasonal cycles in growth and melt (peak-to-trough amplitude of $\sim 1.0 \text{ m}$). The thickness distribution of sea ice controls energy and mass exchanges between the ocean and atmosphere at the surface, and the fresh water fluxes associated with melting ice serve as stabilizing elements in the circulation of the North Atlantic waters. Basin-scale fields of ice thickness are therefore essential for improvements in our estimates of the seasonal and interannual variability in regional mass balance, the freshwater budget of the polar oceans, and the representation of these processes in regional and climate models.

C. Vegetation

Over vegetated surfaces, echo laser waveforms include returns from the top of the canopy, within the canopy, and the ground, which makes laser altimetry very well suited to measuring vegetation height and structure (Fig. 6). However, there are significant differences in sampling and orbit requirements for ice and vegetation measurement objectives. As a result, a separate Earth Science Decadal Survey mission, Deformation Ecosystem Structure and Dynamics of Ice (DESDynI), includes a lidar specifically designed to measure vegetation height, and from that estimate above-ground biomass, while ICESat-2 mainly focuses on ice. Nevertheless, because of the vertical distribution of laser return energy from vegetated surfaces, ICESat-2 is expected to make important contributions to

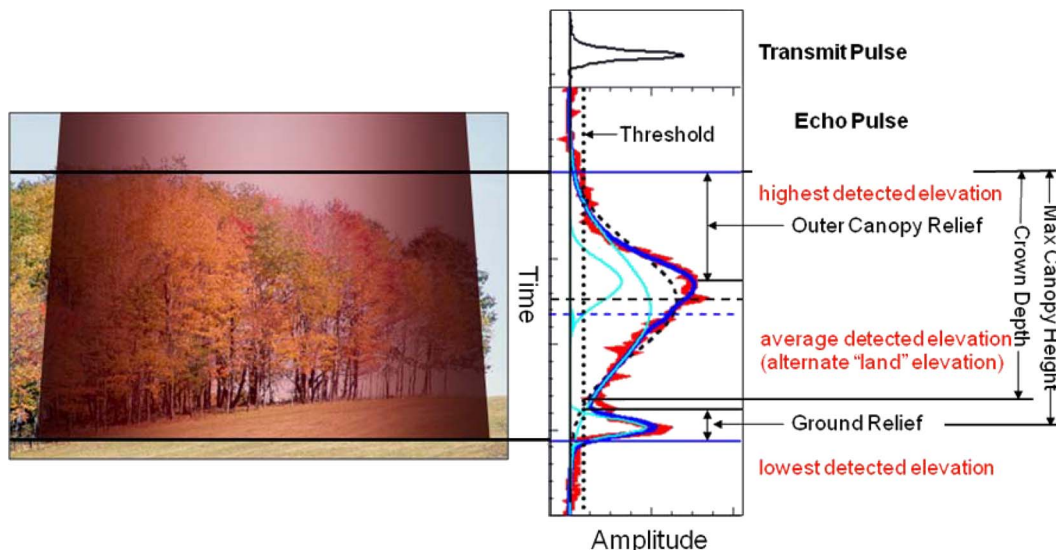


Fig. 6. Depiction of the illumination of trees by an ICESat or ICESat-2 laser spot (left) and the corresponding waveform (right) (from [24]). The waveform shows a clear ground return that is spread by the slope of the ground, the top of the canopy, and returns from within the canopy that are indicative of structure within the crown.

the objectives defined by the vegetation and ecosystem structure science community, specifically an assessment of forest biomass through the measurement of canopy height (Fig. 7). Results from the ICESat mission [25] suggest that extending the ICESat capability to a 91-day continuous measurement could make ICESat-2 capable of producing a vegetation height surface with 3-m accuracy at 1-km spatial resolution, assuming that off-nadir pointing can be used to increase the spatial distribution of observations over terrestrial surfaces.

This sampling, combined with a smaller footprint of 50 m or less, would allow characterization of vegetation at a higher spatial resolution than ICESat, which is expected to provide a new set of global ecosystem applications. These include mapping forest productivity by tracking the growth of individual forest stands, observations of tree phenology, forest disease, and pest outbreaks through associated changes in canopy structure, and the mapping of forest height and aboveground biomass at a scale that approaches one that is appropriate for forest carbon management. Such

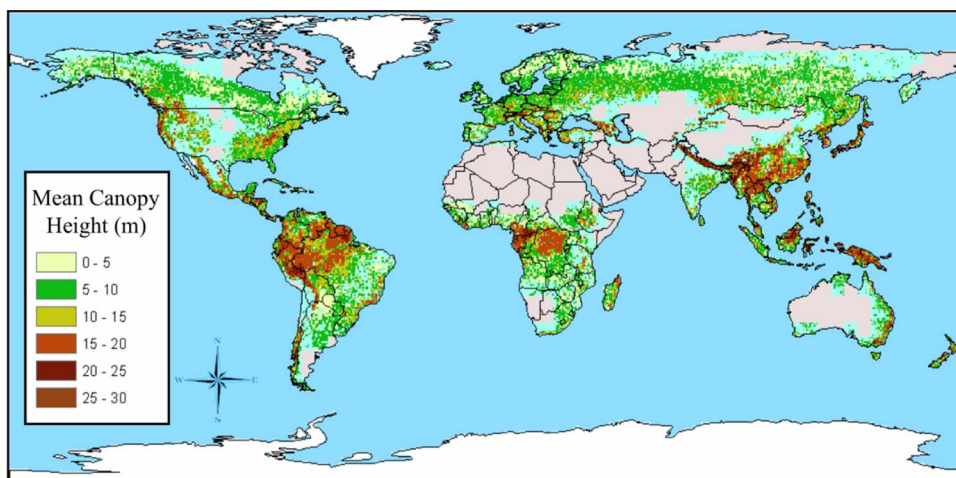


Fig. 7. Global estimates of mean canopy height derived from ICESat. The capability of retrieving tree height with ICESat-2 will contribute to the large-scale biomass assessments.

improvements would enable the global ecosystem community to further constrain the sources and sinks of carbon at regional to continental scales.

D. Other Applications

Satellite laser altimetry provides additional information on a wide range of other Earth surface processes and characteristics, such as mountain glaciers and ice caps [39]–[42], river and lake height [43], [44], ocean tides [45], [46], land surface topography [47], coastal ocean height [44], the geoid and marine gravity field at high latitudes [48], [49], etc. In addition, the atmospheric measurement capability of ICESat-2, even at near-IR wavelengths, will enable global measurements of cloud and aerosol structure to extend the record of these observations beyond those provided by the lasers onboard ICESat [50] and CALIPSO [51]. This demonstrated range of capabilities indicates that ICESat-2 will make important multidisciplinary science contributions; however, it is the ice sheet, sea ice, and vegetation science objectives that drive the mission implementation strategies.

IV. ICESat-2 MISSION CONSIDERATIONS

A. Technical Considerations

The accurate measurement of ice sheet change requires that elevation measurements be made repeatedly over a time interval that is frequent enough to observe the temporal character of changes in a meaningful way. At the same time, the spatial sampling must be sufficiently dense that change can be characterized on the scales at which they vary. To achieve this, the original ICESat mission was placed in a 91-day exact repeat orbit with a 94° inclination at 600 km altitude and used repeat observations of prescribed ground tracks for change determination. ICESat-2 is planned to fly in a similar orbit that repeats these ground tracks, in part because this orbit optimizes the tradeoff between temporal and spatial sampling, providing maximum coverage density while allowing observation opportunities of each ground track once every three months.

Spatial sampling density is of most significance on the outlet glaciers at the ice sheet margins. The spacing between ascending tracks for this orbit is shown as a function of latitude in Table 2. For latitudes greater than 70°, the spacing between ascending and descending tracks is less than 5 km. (On average, the spacing between ascending and descending tracks will be about half of what is reported in Table 2.) This spacing, combined with the fact that most glaciers are not oriented parallel to ascending or descending tracks, means the large majority of outlet glaciers in Antarctica and Greenland will be observed, many on multiple passes, in the 91-day orbit. Even with the compromised 33-day orbits of ICESat, important observations of outlet glacier changes have been made [18]. With

Table 2 Spacing Between Ascending or Descending Ground Tracks in ICESat's 91-Day, 94 Inclination, 600 km Altitude Orbit

Geodetic Latitude (deg)	Track Spacing (km)
0	29.60
5	29.48
10	29.14
15	28.58
20	27.80
25	26.81
30	25.61
35	24.22
40	22.64
45	20.89
50	18.99
55	16.94
60	14.76
65	12.47
70	10.09
75	7.64
80	5.12
85	2.57

the threefold increase in sampling density with ICESat-2 that will be achieved by repeating the 91-day orbit, this capability will be improved upon significantly. In addition, repeating the ICESat orbit enables direct repeat-track comparisons between ICESat and ICESat-2, which facilitates linking the two missions for an extended change assessment that will span more than 15 years.

Achieving repeat track capability imposes very stringent requirements on pointing and orbit control and knowledge. Like its predecessor, ICESat-2 is planned to have the ability to point to reference ground tracks to within 30 m (1-sigma) in order to minimize the separation between observations along each repeat pass. Analysis by the ICESat-2 science definition team [52] indicates that with the 30-m pointing ability, satisfying the change-detection requirements means that the location of the spot on the ground must be known to better than 4.5 m. This level of knowledge is necessary to minimize the effects of surface slope on the elevation change measurement. Also like ICESat, we plan to control the orbit to within 800 m of the reference track to maintain pointing levels of less than 0.1°. Larger values introduce an apparent slope effect that contributes significantly to dh/dt errors. The orbit must also be known to within 2 cm radial distance to satisfy the dh/dt measurement accuracy requirements.

B. Physical Considerations

In addition to these technical considerations, there are physical characteristics of the ice and the atmosphere that influence measurement accuracy. Most significant among these are ice surface roughness and forward-scattering of photons by clouds and blowing snow from a direct measurement perspective and firn density variability for the conversion of elevation change to mass balance.

The horizontal scales of ice sheet roughness vary from millimeters to kilometers with meteorological processes driving small-scale variability, while ice flow and topography of the underlying bedrock control the large-scale variability. The scales most significant for altimetry are on the order of meters to tens of meters for within-footprint measurement accuracy and meters to hundreds of meters for accuracy of interpolation between footprints. One way to minimize noise introduced by surface roughness is by using small footprints at high along-track sampling rates to characterize the surface variability. Another is to use larger footprints to smooth over the roughness elements, which lowers the sampling rate required to achieve a particular accuracy. Because laser life is the primary limiting factor on mission duration and thus science return, strategies that most sparingly use the finite number of laser shots are preferable to those that require high sampling rates for conventional analog pulse lasers.

For ICESat-2, the baseline plan has been for approximately a 50 m footprint size at 50 Hz pulse-repetition frequency (PRF), which provides laser shots spaced at 140 m along-track. For the vast majority of the Greenland and Antarctic ice sheets, 140 m is a reasonable scale over which the elevation can be interpolated [52]. SDT analyses show that footprints of this size and spacing should smooth out the surface roughness characteristics sufficiently, so that ICESat-2 can achieve the desired measurement accuracy at this sampling rate [52]. At 50 Hz, the ICESat-2 along-track sampling would be 20% more dense than that of ICESat.

Previous analyses have shown that forward scattering of photons in clouds leads to pulse broadening and a range bias for surface altimetry. This occurs because the path of photons forward-scattered through clouds from the satellite to the ground and back to the sensor is not direct and, if not accounted for, can bias elevation retrievals by meters [53]. It has been shown [54] that by filtering plus estimating, the ranging errors from the 532 nm data could sufficiently correct ICESat surface elevations to meet all science requirements. Because atmospheric science is not an objective of the ICESat-2 mission, a strategy for dealing with forward scattering is necessary that does not rely on direct atmospheric measurements from a 532 nm laser. For actual ICESat data, cloud-clearing based on the 1064 nm ICESat return signal addresses the largest effects, but a bias of as much as 10 cm or more from clouds and blowing snow remains. For ICESat-2, a means to bring forward scattering errors to below the elevation accuracy requirements is necessary for a 1064 nm altimeter. Reducing the instrument field of view (FOV) can reduce the forward scattering biases significantly, since more of the scattered photons are outside the smaller fields of view. To examine the extent to which reducing the FOV can mitigate forward scattering effects, the SDT analyzed data from several areas in Antarctica (Fig. 8) using an estimated range delay (ERD) from cloud scattering based on ICESat cloud statistics. The range delay was estimated using Monte

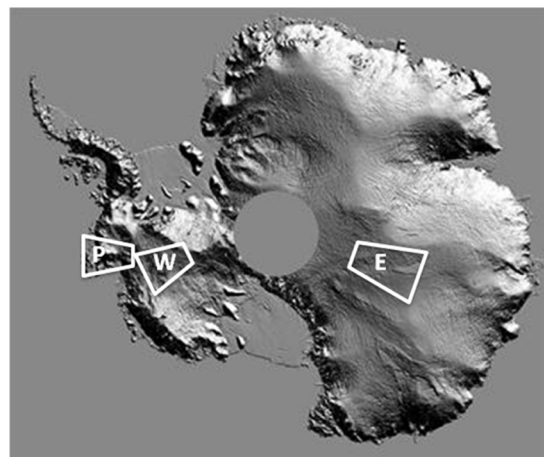


Fig. 8. Areas in Antarctica where analysis of field-of-view effects were examined. The background figure is a shaded-relief digital elevation model of Antarctica derived from ICESat (Dimarzio et al., 2007). The gray circle in the middle shows the “pole-hole” area that is not covered by the 94° inclination of ICESat.

Carlo and analytical radiative transfer calculations using the best available particle and scattering models for ice clouds over ice sheets [53], [55]. The analysis was carried out using accurate cloud data from fall 2003 when the 532 nm channel was operating [52].

We have modeled the approach of reducing the receiver FOV and applying corrections that could be done with ICESat 1064-nm cloud detection. Results are shown in Table 3 for one-month averages over the areas shown in Fig. 8. The estimate of the residual error was based on the analysis of the relative frequency of optically thin clouds detected by the 532-nm channel but undetected by the 1064-nm channel as a function of cloud optical depth retrieved from the 532-nm channel [50]. The error includes those clouds below the level of detection with the 1064-nm-only cloud channel. These analyses indicate that for fields of view on the order of 100–160 μ rad (60 and 100 m on the ground, respectively), the effects of forward scattering on 1064 nm analog laser pulses are reduced to near or within the accuracy requirements. However, in order to reach these accuracies, a cloud and blowing snow detection capability similar to that of the existing ICESat 1064-nm channel would need to be available for ICESat-2. This in turn would place minimum requirements on laser energy that are consistent with those required for altimetry discussed below.

Finally, the primary challenge in converting altimetry observations of ice sheet elevation change to mass balance is in the uncertainty in the density of mass lost or gained. Several models have been developed to account for elevation changes attributable to firn densification [56], [57], which have been instrumental in the interpretation of elevation changes from past and current altimetry missions (e.g., [1], [58], and [59]). Another aspect of that

Table 3 Estimated Range-Delay (ERD) Results for Four Different Fields of View in Different Regions of Antarctica (Shown in Fig. 8). The First Row Shows Analysis of the Average ERD With No Cloud Clearing or Correction With the Effect From Clouds and Blowing Snow Shown Separately. The Second Row Is an Estimated Residual Error After Cloud Clearing Feasible From Direct 1064 nm Cloud Signals

	FOV (μ rad)	500	200	160	100
Pine Island Region	Average ERD Clouds, Bln Sn (cm)	~16, 4	~6, 4	~3.5, 2	~2, .4
	Residual Error Total (cm)	~6	~3.5	~2.5	~1
West Antarctic Ice Sheet Interior	Average ERD Clouds, Blowing Snow (cm)	~12, 12	~4, 8	~2.5, 6	~2, 1.5
	Residual Error Total (cm)	~7	~4	~2.5	~1.5
East Antarctic Ice Sheet Interior	Average ERD Clouds, Bln Sn (cm)	~4, 8	~1.5, 6	~1, 4.5	~1, 1
	Residual Error Total (cm)	~4	~2.5	~1.5	~0.6

conversion, however, is assessing how much of the observed elevation changes in the accumulation zones are dynamically driven and how much are dominated by surface balance. In the case of the former, the conversion of elevation change to mass change assumes the density of ice, while in the case of the latter, the volume lost is assumed to be the density of firn. Observations and model estimates of surface balance and flow characteristics provide important insights into the relative weighting between the two in order to reduce uncertainty. More directly, however, comparisons between mass change estimates derived from the Gravity Recovery and Climate Experiment (GRACE) and elevation changes from altimetry enable estimates of the densities for the volume-to-mass conversions at large spatial scales on the order of 200–500 km, which has been used to constrain higher resolution ICESat observations [14], [59]. GRACE has its own limitations, arising from the large uncertainties related to postglacial rebound, but the combination of ICESat and GRACE is improving our understanding of both ice sheet density and the postglacial rebound. Unfortunately, it is not clear that ICESat-2 and the successor to GRACE will overlap in the current implementation plan of the Decadal Survey. However, the information learned from comparisons between the current ICESat and GRACE missions will be used to improve densification models and our understanding of the dynamic and surface contributions to mass balance. These in turn will inform our interpretation of elevation-change signals from ICESat-2.

C. Mission Duration

A major consideration for the mission implementation is maximizing laser life in order to enable a continuously operating five-year mission. For ice sheets, five years is the minimum necessary to characterize ice sheet interactions with climate, as it is on the order of the shortest time scales of surface balance variability [60], [61]. It is also the absolute minimum time required to examine the responses of outlet glaciers and ice sheets to major

forcings such as the catastrophic collapse of a floating ice shelf or retreat of outlet glacier floating tongues. Responses to these forcings include both the inward propagation of the marginal perturbation effects, which can take years [36], and the time required for outlet glaciers to establish a new quasi-steady-state surface and velocity profile after such perturbations [62]–[65]. Five years of observations will not capture the full evolution of forcing and response in most cases, but sustained, continuous, and detailed observations of this duration or longer will advance the capabilities of ice sheet and outlet glacier models that seek to describe ice-climate interactions and the physics associated with responses to major forcings.

In the case of sea ice, five or more years are also necessary for developing an understanding of the ocean/atmosphere/sea ice exchanges. It has been shown, for example, that the behavior of the anomalies of temperature and salinity in the central Arctic Ocean follows a first-order linear response to the Arctic Oscillation with a time constant of five years and a delay of three years [66]. Ice-climate interactions must be observed through at least a typical cycle of high-frequency climate processes like the Arctic Oscillation in order to characterize ice-climate interactions. Anything shorter will subsample this variability and will alias the ice-change signal that follows from such quasi-periodic climate processes.

As the mission proceeds, mapping of forest height and biomass will be improved as the areas between tracks are filled in and the spatial density of observations increases. A longer mission will also (as with the other application areas) allow a longer period to monitor change in forest height and aboveground biomass due to stand growth, changes in forest health, and recovery from disturbance.

Finally, five years of observation starting in 2015 will provide a sufficiently long period between the earliest ICESat measurements and the latest ICESat-2 measurements to quantify more than 15 years of change. Such a

time span facilitates separation of climatologically significant trends from short-term variability in the combined ICESat/ICESat-2 time series.

Strategies being adopted to maximize laser life include maintaining a low PRF to spread a finite number of shots over a long period and operating at low energy to minimize the stress on the lasers. There are tradeoffs, however, and the advantage of implementing these strategies must be weighed against the need for high energy to penetrate thin and clouds and the need for high PRF to sample surface variability sufficiently. The tradeoffs between PRF and footprint size, and their implications on laser life, have been discussed under Section IV-B, and they suggest that for a single-beam laser system like GLAS on ICESat, a baseline configuration with a footprint size of approximately 50 m and a PRF of 50 Hz (140 m along-track spacing).

Each ICESat laser at initial start-fire operated at approximately 70 mJ. For a similar laser system on ICESat-2, the requirement would be reduced to 50 mJ, assuming a telescope size of 1-m like ICESat carried. ICESat-2 SDT analyses show that at these levels, every 10 mJ reduction in transmit energy corresponds to an average decrease in the amount of surface returns by 2–4% [52]. However, in certain regions such as coastal Antarctica and Greenland and over sea ice, the loss of surface returns can be as much as 15% per 10 mJ of laser energy. While higher energy would be preferable, in order to maximize the amount of surface returns, a reduction to at least 50 mJ is necessary to reduce stress on the lasers. Current laboratory assessments of a modified version of the original ICESat engineering test unit have demonstrated nearly 2.6 billion shots at 50 Hz and 50 mJ with minimal energy loss. At 2 billion shots per laser and 50 Hz, four lasers operating one at a time should support a five-year mission. Configurations considered include as many as six lasers, with the two additional lasers carried primarily for redundancy, but also in part as recognition of the importance of long-term measurements. If all six lasers were to perform at the 2 billion shot level, ICESat-2 could provide more than seven years of measurement at 50 Hz. Additionally, a laser energy of at least 50 mJ will ensure a sufficient cloud and blowing snow detection capability, which is crucial for identifying and filtering altimetry measurements that have been biased by forward scattering.

V. MISSION STATUS

The Decadal Survey categorized its recommended missions into three tiers: near-term, mid-term, and long-term. ICESat-2 is one of four first-tier (near-term) missions recommended for launch as early as 2010. Currently planned for launch in the 2015 time frame, ICESat-2 is still in the early stages of development. However, experiences with ICESat and associated lessons-learned have provided important information that inform the design significantly. These experiences combined with the science require-

ments from the SDT have led to a flow-down from science objectives to measurement requirements to instrument and mission requirements, as shown in Table 4. With the mission only recently entering Phase A, which is when the preliminary design and project plan are developed, a number of important tradeoffs are under consideration to provide the optimum science return. Despite this, the elements of Table 4 present well-understood requirements that provide a solid design foundation.

Fundamental to the success of ICESat-2 is understanding and overcoming the causes of ICESat's premature laser failure (laser 1) and rapid energy degradation (laser 2). The cause of failure for laser 1 was found to be the erosion of gold conductors in the laser diode array due to excessive amount of indium solder. This solder combined with the gold to form nonconducting gold indide, which caused the diode array to stop functioning [67]. The likely cause of rapid energy loss in laser 2 is believed to have been a photodarkening that occurred at and near the laser's frequency doubler [68]. In particular, trace levels of hydrocarbons outgassed from adhesives used in the laser are believed to have interacted with the 532 nm photons. These issues will be addressed on ICESat-2 by eliminating indium from the solder material and possibly pressurizing the housing to avoid outgassing. The nearly 2.6 billion shots to date on the engineering test unit with these mitigation strategies implemented indicate that at least one candidate laser system can achieve five years or more of continuous measurements at 50 Hz and 50 mJ with four or more lasers.

The mid-decade launch date, coupled with the fact ICESat is no longer collecting altimetry data, will lead to a multiyear gap in satellite laser altimetry measurements between ICESat and ICESat-2. In the intervening period, NASA is implementing Operation IceBridge, a series of airborne campaigns in Greenland, Antarctica, and their surrounding seas, designed to survey high-priority areas with a range of instrumentation that includes airborne laser altimetry. IceBridge observations will provide some continuity of data between missions for these high-priority targets and collect data in support of model development.¹

In addition, the European Space Agency's satellite radar altimeter CryoSat-2 is scheduled for launch in early 2010. Cryosat-2 is a three-year mission that is also intended to measure ice sheet changes and sea ice freeboard height, but it will do so using radar altimetry at up to 250-m along-track resolution based on an interferometric processing technique [69]. As a radar altimeter, Cryosat-2 will provide coverage under cloudy conditions. On sea ice, the penetration characteristics of radar into snow that may overlie sea ice make its returns more likely to be from the interface between the ice and snow, rather than from the snow surface itself. In other words, it will likely measure F_1 in Fig. 4, rather than F . Since the presence of snow on

¹Details can be found at <http://www.espo.nasa.gov/oib/>.

Table 4 General Flowdown From Science Goals to Implementation Requirements

Science Goals	Science Requirements	Measurement Requirements	Instrument Functional Requirements	Mission Functional Requirements
<p><u>Ice Sheets</u></p> <p>Quantify polar ice sheet mass balance to determine contributions to current and recent sea level change and impacts on ocean circulation</p> <p>Determine seasonal cycle of ice sheet changes</p> <p>Determine topographic character of ice sheet changes to assess mechanisms driving that change and constrain ice sheet models</p>	<p>Annual elevation change of 0.2 cm/yr over entire ice sheet</p> <p>Surface elevation change of 25 cm/yr annually in 100 km² areas and along linear distances of 1 km</p> <p>Resolve winter and summer ice sheet elevation change to 2.5 cm over 25x25 km² areas</p> <p>Continuous observations through for at least 5 years</p> <p>Direct comparability to ICESat-I measurements for 15-year dh/dt</p>	<p>Ability to penetrate optically thin clouds</p> <p>Precise repeatability of ground tracks</p> <p>Repeat sampling 4x per year, uniformly spaced in time</p> <p>Slope information in the cross-track direction</p> <p>Continuous measurements for no less than 5 years</p>	<p>4.5 m pointing knowledge</p> <p>5 years continuous operation with 7-year goal</p> <p>Measurement capability in the cross-track direction within the vicinity of the primary beam</p> <p>Surface reflectivity capability of 5% to enable characterization of snow conditions for gain and range corrections</p>	<p>Orbit parameters comparable to those of ICESat (600 km altitude; 94 deg. incl., 91-day repeat).</p> <p>10 arcsec (30-m) pointing control</p> <p>1.5 arcsec (4.5-m) pointing knowledge</p> <p>2 cm radial orbit accuracy requirement</p> <p>5 year continuous operation with 7-year goal</p>
<p><u>Sea Ice</u></p> <p>Estimate sea ice thickness to examine ice/ocean/atmosphere exchanges of energy, mass and moisture</p>	<p>Discriminate freeboard from surrounding ocean level to within 3 cm</p> <p>Capture seasonal evolution of sea ice cover on 25 x 25 km scales</p>	<p>Vertical precision of <2 cm between leads and sea ice freeboard height</p> <p>Monthly near-repeat coverage of Arctic and Southern Oceans at 25 x 25 km scales</p> <p>Coverage up to at least 86 deg. latitude</p>	<p>Telescope FOV of 100 m (160 μrad) or better to minimize atmospheric forward-scattering effects</p> <p>Atmospheric vertical resolution of 75 km to enable atmospheric corrections plus studies of clouds</p>	<p>91 day repeat orbit to capture seasonal effects and maximize comparability to ICESat for trend detection</p>
<p><u>Vegetation</u></p> <p>Estimate Large Scale Biomass in Support of DESDynI Science Requirements</p>	<p>Produce a global vegetation height surface with 3-m accuracy at 1-km resolution</p>	<p>Ability to point between nadir ground tracks on every ascending and descending pass to fill in gaps between tracks every km over non-ice-covered land</p>		

sea ice adds uncertainty to the thickness estimate (for lasers by changing the total column density used to convert freeboard to thickness, and for radar, by lowering the ice/snow interface under the weight of the snow), it must be

accounted for in either measurement. Currently, this is estimated using snow climatology [37], snowfall from meteorological fields [9], or derived snow fields from passive microwave data [22]. If there is overlap between

ICESat-2 and Cryosat-2, however, differences in freeboard height over the same locations will presumably provide a direct measure of snow height. Also, with ICESat-2's smaller laser footprint, it should be able unambiguously sample smaller leads than Cryosat-2. A comparison between the two should help quantify the lead size identifiable by Cryosat-2 and the implications for freeboard estimates for both measurement approaches.

On ice sheets, Cryosat-2's all-weather capability will provide more observations under cloudy conditions that are often persistent in some of the coastal areas of Greenland and Antarctica. However, because it carries a Ku-band radar, variable penetration into firm adds an uncertainty to the elevation change retrievals that is not inherent in the laser observations. Moreover, the repeat-track capability of ICESat-2 will allow change detection along linear tracks, providing much greater detail in the along-track direction than can be achieved with the traditional crossover analysis, as will be done with Cryosat-2.

Though the measurement technologies are very different between ICESat/ICESat-2 and Cryosat-2, each is a valuable complement to the other, and together they will provide crucial data on ice sheet and sea ice changes over most of the 2003-2020 time period. The greatest benefits will be realized if there is significant overlap between Cryosat-2 and ICESat-2 for a year or more, which will allow cross-calibration between the two missions.

VI. MISSION CONFIGURATION OPTIONS

Three basic candidate mission configuration options have been examined for ICESat-2. The simplest employs a single-beam near-infrared laser approach that would be very similar to ICESat (Fig. 1). Like ICESat, it would carry multiple lasers with only one operating at a time. Because it is not possible to overlay each repeat track exactly on top of one another, along-track and cross-track offsets in the beam locations between repeat tracks on the sloped ice sheet surface can introduce significant errors in the elevation change calculations. These errors manifest themselves as "apparent" elevation changes between repeat passes due to the component of surface slope in either the along-track or the cross-track direction. Along-track slopes can be estimated from adjacent consecutive measurements, but cross-track slopes must employ data from multiple passes (Fig. 9). Correcting for this in repeat-track analyses usually employs a simultaneous solution of cross-track slope (α) and elevation change (dh/dt) according to the following formula:

$$H(x, \alpha, t) = H(t_1) + x \tan(\alpha) + t(dh/dt) \quad (1)$$

where H is the surface height at the reference track at time t (with t_1 being the time of the first measurement) and x is a horizontal distance from the reference track.

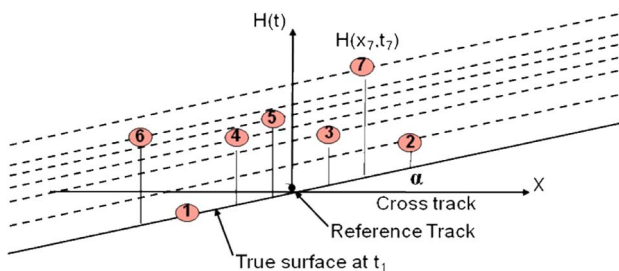


Fig. 9. Representation of a rising ice sheet surface that is observed by seven individual ground tracks that are oriented perpendicular to the page. Each number represents a different observation period, and the diagonal line passing through that number represents the height of the sloped surface at the time of observation. Each observation is offset some distance (x) from the reference track (the black dot at the intersection of the "Cross-track" and " $H(t)$ " axes).

As a result, for a single-beam configuration, repeat-track elevation change can only be determined after a sufficient number of observations has been acquired, in order to solve (1). At a minimum, this is four observations, but in practice, analyses of ICESat data have shown that achieving the required elevation change accuracy requires ten or more. In coastal regions, where a vast majority of ice loss occurs, surface signals are not retrieved for approximately half of the passes, due to extinction under persistent optically thick atmospheric conditions [70]. Under these circumstances, approximately five years of measurements are needed on average before the required change-detection accuracy can be achieved. Moreover, assessing the variability in dh/dt in this way requires the assumption that slopes are constant throughout the mission. This constant-slope assumption is reasonable for the ice sheet interior, but near the margins, slopes will likely change considerably throughout the mission, especially following major change events. Thus capturing changes in these crucial areas of the ice sheets requires the simultaneous measurement of cross-track slope and elevation. This has led the ICESat-2 SDT to recommend the incorporation of a cross-track measurement capability in order to enable the direct observation of slope and elevation and their time-varying changes.

The geometry of any cross-track implementation has to take into account that the spacecraft may not remain in the same orientation with respect to its velocity vector throughout the year. At an inclination of 94° , ICESat-2, like ICESat, will not be sun-synchronous. To maintain sufficient illumination of its solar panels to meet power requirements, ICESat executes a series of 90° yaw maneuvers twice each year, such that during half the year, the solar panels are aligned perpendicular to the velocity vector (referred to as airplane mode) and half the year, they are aligned parallel to the velocity vector (referred to as sailboat mode). Cross-track approaches under consideration are those that can accommodate both airplane and sailboat mode.

For ICESat-2, two candidate options for acquiring cross-track measurements have been studied. The first is a quad-beam approach (Fig. 10). Under this configuration, a diffractive optical element would be used to divide the main beam into four separate beams, oriented to the corners of a several-kilometer-wide square centered on the nadir point. Under normal operations, the square of spots would be rotated by about 2° relative to the spacecraft velocity vector, so that the leading pair of beams would be offset cross-track from the trailing pair of beams, and each pair of beams would define the surface slope along a 140-m swath. As an example, a $4\text{ km} \times 4\text{ km}$ square would acquire two pairs of measurements, one along the ICESat reference track and the other offset by 4 km (approximately 0.4°).

This approach relies on two points in a pass to characterize the cross-track slope. It also increases spatial coverage by laying down tracks between reference tracks. The quad-beam approach, however, significantly reduces the amount of laser energy in each beam, which in turn reduces the number of successful measurements that would be acquired with each beam. A telescope that is significantly larger than the 1-m telescope used on ICESat could partly mitigate the effects of reduced energy, as could

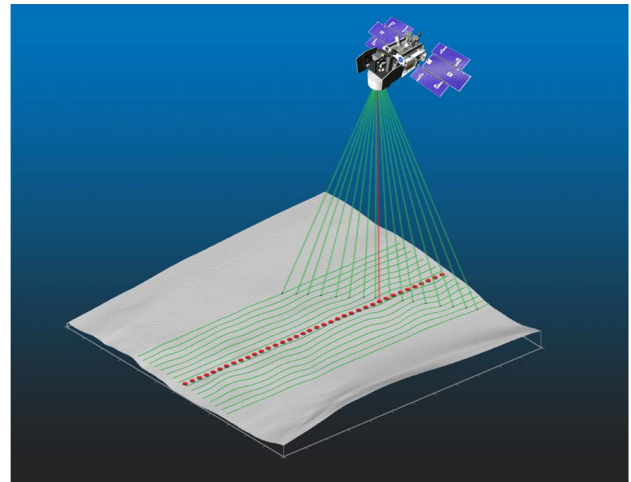


Fig. 11. Representation of a sampling structure for the 16-beam high-repetition-rate photon-counting approach.

fewer beams (two or three rather than four). Ultimately, however, the impact on overall measurement capability of each beam must be traded against the value of the cross-track information and increased sampling. The quad-beam configuration, or its two- or three-beam variant, could also be achieved with multiple lasers, but the simultaneous use of multiple lasers has a significant impact on the power and thermal requirements as well as mission lifetime.

The second cross-track approach adds a different type of laser and detector system, a micropulse lidar [71], to measure surface elevations over a swath on either side of the main beam. This cross-track channel (CTC) uses a high-pulse-repetition laser with its output split into as many as 16 cross-track beams with small (10 m) footprints on tracks parallel to the main beam (Fig. 11). The number of transmitted photons per second from the CTC laser is on the same order as that from the main-beam laser, but the CTC photons are more widely distributed to provide more information on the surface topography. A high laser repetition rate of 10 kHz produces overlapping footprints that are spaced by about 0.70 m along-track, as shown in Fig. 12. The laser output energy is selected such that the photon-counting detector will detect one photon from each overlapping footprint with a probability of about 80%. A short laser pulse width of about 1 ns enables the determination of surface elevations to an accuracy of about 10 cm. The micropulse CTC laser currently under consideration includes a frequency doubler, so efficient photon-counting detectors sensitive to green wavelengths can be used. This approach has the significant advantage of dense along track coverage and the ability to produce more beams, since the number of beams is driven by the probability of detecting the return of a single photon in each footprint. This increased sampling plus the small 10-m footprints are advantageous for sea ice, as they would

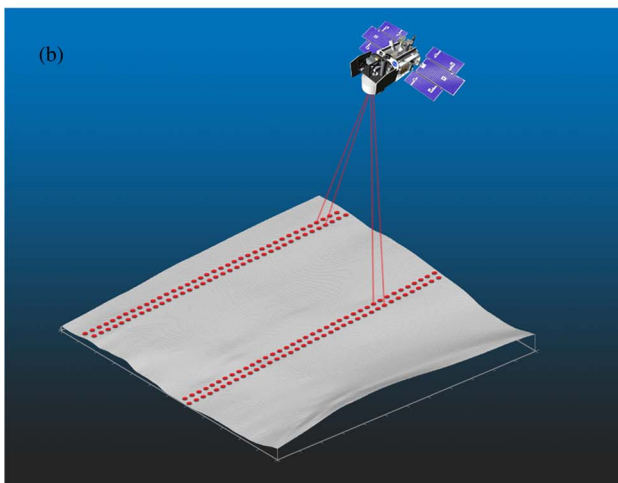
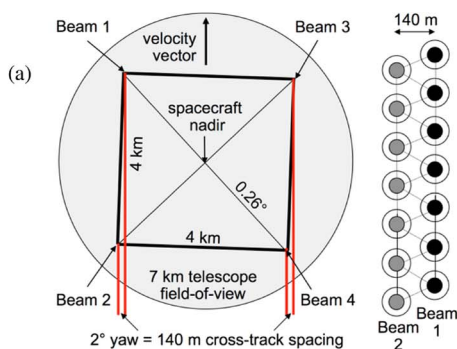


Fig. 10. Representation of (a) a configuration and (b) a sampling structure for the quad-beam approach. In (b), each pair of beams is spaced 140 m apart, and there is 4 km of separation between pairs.

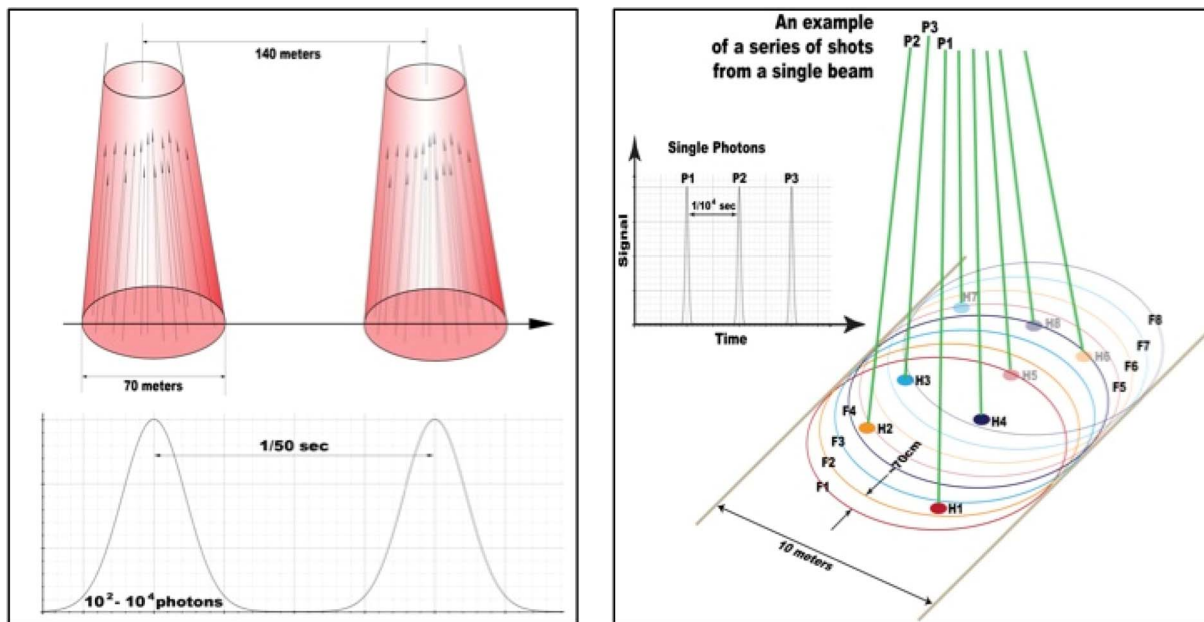


Fig. 12. Depiction of a conventional analog laser return signal of a 70-m footprint laser at (left) 50 Hz and a 10 kHz photon-counting digital return signal. In the analog case, the photons are collected by the receiving telescope to produce a waveform. In the digital case, single photons are detected from within 10-m-diameter circles spaced incrementally at 70 m. In the digital approach, uncertainty arises from not knowing where within that 10-m circle the photon was returned from, so along-track averaging is employed to improve measurement accuracy.

enable the detection of smaller leads, which would improve freeboard measurement accuracy. At green wavelengths, there is the added complexity of the penetration into the leads, which will require filtering of subsurface returns. In the combined micropulse/analog configuration shown in Fig. 11, any ambiguities can be further resolved through cross-calibration with a near-IR beam.

The CTC approach also has the potential to improve measurements of vegetation canopy heights along each cross-track beam using algorithms that calculate the along-track surface elevation profile. Calculation of the surface profile enables construction of above-surface canopy height distributions independent of surface slope over lengths greater than the 10 m footprint size. These canopy height distributions can also be constructed over various along-track distances (e.g., 100–500 m) corresponding to the appropriate decorrelation length scale of the various vegetation types. The extent to which this approach will support vegetation and ecosystem science objectives is currently under investigation.

A fully capable micropulse lidar system can potentially serve both the primary and cross-track measurement functions, eliminating the need for the analog pulse lidar; however, the two are most effective as complementary measurements. The analog pulse laser is familiar and has significant heritage, in terms of both space flight and algorithms. The micropulse lidar offers potentially excellent sampling capabilities; however, it is a novel approach with a limited history. Flying both lasers simultaneously would provide an important cross-

calibration opportunity that would enable effective merging the strengths of the two.

VII. SUMMARY AND CONCLUSIONS

The Earth’s ice cover has experienced substantial and unexpected changes in the last few decades, and satellite laser altimetry has been demonstrated as a very useful tool for examining and understanding these changes. Because of the severely compromised performance of two of its three lasers, the original ICESat mission never realized its full potential. ICESat has, however, provided many important insights into the value of laser altimetry for ice sheet, sea ice, vegetation, and other measurements, and has provided a unique initial time series to help assess the state of polar ice. ICESat-2 will carry this capability forward into the future and provide continuous detailed observations of the polar ice and vegetation with three or more the spatial coverage of ICESat. In so doing, it will enable scientists to quantify the seasonal and annual contributions of the ice sheets to sea level rise, the rate of mass balance changes of Arctic and Antarctic sea ice, and the amount of global biomass, with unprecedented accuracy.

In the case of ice sheet changes, ICESat-2 will go beyond these historic assessments and provide important and unique insights into the processes that control ice sheet mass balance based on observations of their topographic expressions. These observations will support the development of models designed to predict the contributions of the

Greenland and Antarctic ice sheets to sea level in the coming decades. With respect to sea ice, ICESat-2 will provide the critical third dimension that is needed to understand the nature and distribution of change. When appropriately incorporated into models along with complementary oceanographic and atmospheric measurements, these observations will help scientists understand the processes that control sea ice change and the implications for future climate, filling a significant gap in our climate prediction capability. For vegetation, ICESat-2 will contribute to large-scale biomass assessment, helping us understand the global distribution of carbon on land, which will complement those of the DESDynI mission, whose orbit and laser system is more specifically targeted at vegetation and ecosystem science objectives. ICESat-2 will be capable of supporting other science disciplines as well, including hydrology, oceanography, geology, atmospheric science, etc., through its precise elevation measurement capability.

Note added in proof: With launch not scheduled until ~2015, the final configuration of the ICESat-2 mission is

still being refined. However, based on the capabilities demonstrated by ICESat and planned improvements that follow from our experiences with that mission, ICESat-2 is expected to provide critical observations for addressing some of today's most important challenges in Earth science.

Since the time this paper was accepted, programmatic and scientific considerations have resulted in the selection of the micropulse lidar with no analog central beam as the implementation approach for ICESat-2. As a result, the micropulse cross-track channel will serve both the primary measurement function and the cross-track measurement function. ■

Acknowledgment

The authors acknowledge the three anonymous reviewers whose comments were helpful in the revision of this paper. The authors also wish to thank David Hancock for providing detailed information on operational characteristics of the ICESat mission.

REFERENCES

- [1] R. Thomas, E. Frederick, W. Krabill, S. Manizade, and C. Martin, "Progressive increase in ice loss from Greenland," *Geophys. Res. Lett.*, vol. 33, no. 10, 2006.
- [2] P. Lemke, J. Ren, R. B. Alley, I. Allison, J. Carrasco, G. Flato, Y. Fujii, G. Kaser, P. Mote, R. H. Thomas, and T. Zhang, "Observations: Changes in snow, ice and frozen ground," in *Climate Change 2007: The Physical Science Basis. Contribution of Working Group I to the Fourth Assessment Report of the Intergovernmental Panel on Climate Change*. Cambridge, U.K.: Cambridge Univ. Press, 2007, pp. 337–383.
- [3] E. Rignot, J. E. Box, E. Burgess et al., "Mass balance of the Greenland ice sheet from 1958 to 2007," *Geophys. Res. Lett.*, vol. 35, no. 20, Oct. 22, 2008.
- [4] I. Joughin, W. Abdalati, and M. Fahenstock, "Large fluctuations in speed on Greenland's Jakobshavn Isbrae Glacier," *Nature*, vol. 432, pp. 608–610, 2004.
- [5] E. Rignot and P. Kanagaratnam, "Changes in the velocity structure of the Greenland ice sheet," *Science*, vol. 311, no. 5763, pp. 986–990, Feb. 17, 2006.
- [6] A. Luckman, T. Murray, R. de Lange, and E. Hanna, "Rapid and synchronous ice-dynamic changes in East Greenland," *Geophys. Res. Lett.*, vol. 3, no. 33, 2006.
- [7] E. Rignot, "Changes in ice dynamics and mass balance of the Antarctic ice sheet," *Phil. Trans. Royal Soc. A, Math. Phys. Eng. Sci.*, vol. 364, no. 1844, pp. 1637–1655, Jul. 15, 2006.
- [8] J. Stroeve, M. M. Holland, W. Meier et al., "Arctic sea ice decline: Faster than forecast," *Geophys. Res. Lett.*, vol. 34, no. 9, May 1, 2007.
- [9] R. Kwok, G. F. Cunningham, M. Wensnahan, I. Rigor, H. J. Zwally, and D. Yi, "Thinning and volume loss of the Arctic Ocean sea ice cover: 2003–2008," *J. Geophys. Res., Oceans*, 2009.
- [10] T. A. Scambos, J. A. Bohlander, C. A. Shuman, and P. Skvarca, "Glacier acceleration and thinning after ice shelf collapse in the Larsen B embayment," *Antarctica, Geophys. Res. Lett.*, vol. 31, 2004.
- [11] E. Rignot, G. Casassa, P. Gogineni, W. Krabill, A. Rivera, and R. Thomas, "Accelerated ice discharge from the Antarctic Peninsula following the collapse of Larsen B ice shelf," *Geophys. Res. Lett.*, vol. 31, 2004.
- [12] W. B. Krabill, E. Hanna, P. Huybrechts, W. Abdalati, J. Cappelin, B. Csatho, E. B. Frederick, S. Manizade, C. Martin, J. Sonntag, R. Swift, R. H. Thomas, and J. Yungel, "Greenland ice sheet: Increased coastal thinning," *Geophys. Res. Lett.*, vol. 31, no. 24, 2004.
- [13] H. J. Zwally, M. Giovinetto, J. Li, H. G. Cornejo, M. A. Beckley, A. C. Brenner, J. L. Saba, and D. Yi, "Mass changes of the Greenland and Antarctic ice sheets and shelves and contributions to sea level rise 1992–2002," *J. Glaciol.*, vol. 51, no. 175, pp. 509–527, 2005.
- [14] D. C. Slobbe, P. Ditmar, and R. C. Lindbergh, "Estimating the rates of mass change, ice volume change and snow volume change in Greenland from ICESat and GRACE data," *Geophys. J. Int.*, vol. 176, pp. 95–106, 2008.
- [15] D. J. Cavalieri and C. L. Parkinson, "Antarctic sea ice variability and trends, 1979–2006," *J. Geophys. Res., Oceans*, vol. 11, no. C7, Jul. 1, 2008.
- [16] C. A. Shuman, H. J. Zwally, and B. E. Schutz, "ICESat Antarctic elevation data: Preliminary precision and accuracy assessment," *Geophys. Res. Lett.*, vol. 33, no. 7, 2006.
- [17] H. J. Zwally, R. Schutz, W. Abdalati, J. Abshire, C. Bentley, J. Bufton, D. Harding, T. Herring, B. Minster, S. Palm, J. Spinirne, and R. Thomas, "ICESat's laser measurements of polar ice, atmosphere, ocean, and land," *J. Geodyn.*, vol. 34, no. 4, pp. 405–445, 2002.
- [18] H. D. Pritchard, R. J. Arthern, D. G. Vaughan, and L. A. Edwards, "Extensive dynamic thinning on the margins of the Greenland and Antarctic ice sheets," *Nature*, 2009.
- [19] I. M. Howat, B. E. Smith, I. Joughin, and T. A. Scambos, "Rates of Southeast Greenland ice volume loss from combined ICESat and ASTER observations," *Geophys. Res. Lett.*, vol. 35, 2008.
- [20] R. Kwok, H. J. Zwally, and D. H. Yi, "ICESat observations of Arctic sea ice: A first look," *Geophys. Res. Lett.*, vol. 31, no. 16, Aug. 18, 2004.
- [21] R. Kwok, G. F. Cunningham, H. J. Zwally et al., "Ice, cloud, and land elevation satellite (ICESat) over Arctic sea ice: Retrieval of freeboard," *J. Geophys. Res., Oceans*, vol. 112, no. C12, Dec. 21, 2007.
- [22] H. J. Zwally, D. H. Yi, R. Kwok et al., "ICESat measurements of sea ice freeboard and estimates of sea ice thickness in the Weddell Sea," *J. Geophys. Res., Oceans*, vol. 113, no. C2, Feb. 19, 2008.
- [23] S. L. Farrell, S. W. Laxon, and D. C. McAdoo, "Five years of Arctic sea ice freeboard measurements from the ice, cloud and land elevation satellite," *J. Geophys. Res. Oceans*, vol. 114, 2009.
- [24] D. J. Harding and C. C. Carabajal, "ICESat waveform measurements of within-footprint topographic relief and vegetation vertical structure," *Geophys. Res. Lett.*, vol. 32, 2005.
- [25] M. A. Lefsky, M. Keller, Y. Pang, P. B. de Camargo, and M. O. Hunter, "Revised method for forest canopy height estimation from geoscience laser altimeter system waveforms," *J. Appl. Remote Sens.*, vol. 1, no. 013537, 2007.

- [26] A. L. Neuenschwander, "Evaluation of waveform deconvolution and decomposition retrieval algorithms for ICESat/GLAS data," *Can. J. Remote Sens.*, vol. 34, pp. S240–S246, 2008, suppl. 2.
- [27] Y. Pang, M. Lefsky, H. E. Andersen, M. E. Miller, and K. Sherrill, "Validation of the ICESat vegetation product using crown-area-weighted mean height derived using crown delineation with discrete return lidar data," *Can. J. Remote Sens.*, vol. 34, pp. S471–S484, 2008, suppl. 2.
- [28] J. A. B. Rosette, P. R. J. North, and J. C. Suarez, "Vegetation height estimates for a mixed temperate forest using satellite laser altimetry," *Int. J. Remote Sens.*, vol. 29, no. 5, pp. 1475–1493, 2008.
- [29] J. Boudreau, R. F. Nelson, H. A. Margolis, A. Beaudoin, L. Guindon, and D. S. Kimes, "Regional aboveground forest biomass using airborne and spaceborne LIDAR in Quebec," *Remote Sens. Environ.*, vol. 112, no. 10, pp. 3876–3890, 2008.
- [30] R. Nelson, K. J. Ranson, G. Sun, D. S. Kimes, V. Kharuk, and P. Montesano, "Estimating Siberian timber volume using MODIS and ICESat/GLAS," *Remote Sens. Environ.*, vol. 113, no. 3, pp. 691–701, 2009.
- [31] H. A. Fricker, T. A. Scambos, R. Bindshadler, and L. Padman, "An active subglacial water system in West Antarctica mapped from space," *Science*, vol. 315, no. 5818, pp. 1544–1548, 2007.
- [32] H. A. Fricker and T. Scambos, "Connected subglacial lake activity on lower Mercer and Whillans ice streams, West Antarctica, 2003–2008," *J. Glaciol.*, vol. 55, no. 190, pp. 303–315, 2009.
- [33] B. Smith, H. A. Fricker, I. Joughin, and S. Tulaczyk, "An inventory of active subglacial lakes in Antarctica detected by ICESat (2003–2008)," *J. Glaciol.*, in press.
- [34] National Research Council, *Earth Science and Applications From Space: National Imperatives for the Next Decade and Beyond*. Washington, DC: National Academies Press, Sep. 28, 2007.
- [35] W. Abdalati, W. Krabill, E. Frederick, S. Manizade, C. Martin, J. Sonntag, R. Swift, R. Thomas, W. Wright, and J. Yungel, "Near-coastal thinning of the Greenland ice sheet," *J. Geophys. Res. Atmos.*, vol. 106, no. D24, pp. 33 729–733 742, 2001.
- [36] R. H. Thomas, W. Abdalati, W. B. Krabill, S. Manizade, and K. Steffen, "Investigation of surface melting and dynamic thinning of Jakobshavn Isbrae, Greenland," *J. Glaciol.*, vol. 49, no. 165, pp. 231–239, 2003.
- [37] S. Laxon, N. Peacock, and D. Smith, "High interannual variability of sea ice thickness in the Arctic Region," *Nature*, vol. 425, no. 6961, pp. 947–950, Oct. 30, 2003.
- [38] K. A. Giles, S. W. Laxon, and A. L. Ridout, "Circumpolar thinning of Arctic sea ice following the 2007 record ice extent minimum," *Geophys. Res. Lett.*, vol. 35, 2008.
- [39] J. M. Sauber, J. B. Molnia, C. Carabaja, S. Luthcke, and R. Musket, "Ice elevations and surface change on the Malaspina Glacier, Alaska," *Geophys. Res. Lett.*, vol. 32, no. 23, 2005.
- [40] E. Berthier and T. Toutin, "SPOT5-HRS digital elevation models and the monitoring of glacier elevation changes in North-West Canada and South-East Alaska," *Remote Sens. Environ.*, vol. 112, no. 5, pp. 2443–2454, 2008.
- [41] W. A. Sneed, R. L. Hook, and G. S. Hamilton, "Thinning of the south dome of Barnes ice cap, Arctic Canada, over the past two decades," *Geology*, vol. 36, no. 1, pp. 71–74, 2008.
- [42] A. Käab, "Glacier volume changes using ASTER satellite stereo and ICESat GLAS laser altimetry. A test study on Edgeøya, Eastern Svalbard," *IEEE Trans. Geosci. Remote Sens.*, vol. 46, no. 10, pp. 2823–2830, 2008.
- [43] J. W. Chipman and T. M. Lillesand, "Satellite-based assessment of the dynamics of new lakes in Southern Egypt," *Int. J. Remote Sens.*, vol. 28, no. 19, pp. 4365–4379, 2007.
- [44] T. J. Urban, B. E. Schutz, and A. L. Neuenschwander, "A Survey of ICESat coastal altimetry applications: Continental Coast, open ocean island, and inland river," *Terr. Atmos. Ocean. Sci.*, vol. 19, no. 1–2, pp. 1–19, Apr. 2008.
- [45] L. Padman, L. Erofeeva, and H. A. Fricker, "Improving Antarctic tide models by assimilation of ICESat laser altimetry over ice shelves," *Geophys. Res. Lett.*, vol. 35, 2008.
- [46] R. D. Ray, "A preliminary tidal analysis of ICESat laser altimetry: Southern Ross Ice Shelf," *Geophys. Res. Lett.*, vol. 3, no. 2, Jan. 23, 2008.
- [47] C. C. Carabajal and D. J. Harding, "SRTM C-band and ICESat laser altimetry elevation comparisons as a function of tree cover and relief," *Photogram. Eng. Rem. S.*, vol. 72, no. 3, pp. 287–298, Mar. 2006.
- [48] R. Forsberg and H. Skourup, "Arctic ocean gravity, geoid and sea-ice freeboard heights from ICESat and GRACE," *Geophys. Res. Lett.*, vol. 32, no. 21, Nov. 4, 2005.
- [49] D. C. McAdoo, S. L. Farrell, S. W. Laxon, H. J. Zwally, D. Yi, and A. L. Ridout, "Arctic ocean gravity field derived from ICESat and ERS-2 Altimetry: Tectonic implications," *J. Geophys. Res.*, vol. 113, 2008.
- [50] J. D. Spinhirne, S. P. Palm, W. D. Hart, D. L. Hlavka, and E. J. Welton, "Cloud and aerosol measurements from GLAS: Overview and initial results," *Geophys. Res. Lett.*, vol. 32, no. 22, 2005.
- [51] D. M. Winker, W. H. Hunt, and M. J. McGill, "Initial performance assessment of CALIOP," *Geophys. Res. Lett.*, vol. 34, 2007.
- [52] W. Abdalati et al., "Report of the ad-hoc science definition team for the Ice Cloud and Land Elevation Satellite-II (ICESat-II), 65 pp. [Online]. Available: http://cires.colorado.edu/~waleed/aSDT_Final_Report_11-20-2008.pdf
- [53] D. P. Duda, J. D. Spinhirne, and E. W. Eloranta, "Atmospheric multiple scattering effects on GLAS altimetry—Part I: Calculations of single path bias," *IEEE Trans. Geosci. Remote Sens.*, vol. 39, pp. 92–101, 2001.
- [54] A. Mahesh, J. D. Spinhirne, D. P. Duda, and E. W. Eloranta, "Atmospheric multiple scattering effects on GLAS altimetry—Part II: Analysis of expected errors in Antarctic altitude measurements," *IEEE Trans. Geosci. Remote Sens.*, vol. 40, pp. 2353–2362, 2002.
- [55] Y. Yang, A. Marshak, T. Várnai, W. Wiscombe, and P. Yang, "Uncertainties in ice sheet altimetry from a space-borne 1064 nm single channel lidar due to undetected thin clouds."
- [56] R. A. Arthern and D. J. Wingham, "The natural fluctuations of firn densification and their effect on the geodetic determination of ice sheet mass balance," *Climatic Change*, vol. 30, no. 4, pp. 605–624, 1998.
- [57] J. Li and H. J. Zwally, "Modeled seasonal variations of firn density induced by steady-state surface air-temperature cycle," *Ann. Glaciol.*, vol. 34, pp. 299–302.
- [58] D. J. Wingham, A. Shepherd, A. Muir, and G. J. Marshall, "Mass balance of the Antarctic ice sheet," *Phil. Trans. Royal Soc. A*, vol. 364, pp. 1627–1635, 2006.
- [59] B. Gunter, T. Urban, R. Riva, M. Helsen, R. Harpold, S. Poole, P. Nagel, B. Schutz, and B. Tapley, "A comparison of coincident GRACE and ICESat data over Antarctica," *J. Geodyn.*, 2009.
- [60] J. E. Box, D. H. Bromwich, B. A. Veenhuis, L.-S. Bai, J. C. Stroeve, J. C. Rogers, K. Steffen, T. Haran, and S. H. Wang, "Greenland ice sheet surface mass balance variability (1988–2004) from calibrated Polar MM5 output," *J. Climate*, vol. 19, no. 12, pp. 2783–2800, 2006.
- [61] A. J. Monaghan, D. H. Bromwich, and S. H. Wang, "Recent trends in Antarctic snow accumulation from Polar MM5," *Phil. Trans. Royal Soc. A*, vol. 364, pp. 1683–1708, 2006.
- [62] A. J. Payne, "Dynamics of the Siple Coast ice streams, West Antarctica: Results from a thermomechanical ice sheet model," *Geophys. Res. Lett.*, vol. 25, pp. 3173–3176, 1998.
- [63] I. M. Howat, I. Joughin, M. Fahnestock, B. E. Smith, and T. A. Scambos, "Synchronous retreat and acceleration of southeast Greenland outlet glaciers 2000–06: Ice dynamics and coupling to climate," *J. Glaciol.*, vol. 54, no. 187, pp. 646–660, 2008.
- [64] I. Joughin, I. M. Howat, M. Fahnestock, B. Smith, W. B. Krabill, R. Alley, H. Stern, and M. Truffer, "Continued evolution of Jakobshavn Isbrae following its rapid speedup," *J. Geophys. Res., Earth*, vol. 133, no. 113, 2008.
- [65] F. M. Nick, A. Vieli, I. M. Howat, and I. Joughin, "Large-scale changes in Greenland outlet glacier dynamics triggered at the terminus," *Nat. Geosci.*, vol. 2, pp. 110–114, 2009.
- [66] J. Morison, M. Steele, and T. Kikuchi, "Relaxation of central Arctic Ocean hydrography to pre-1990s climatology," *Geophys. Res. Lett.*, vol. 33, no. 17, 2006, L17604.
- [67] R. Kichak, *Independent GLAS Anomaly Review Board executive summary*, Nov. 2003, p. 4. [Online]. Available: <http://icesat.gsfc.nasa.gov/docs/IGARB.pdf>
- [68] G. R. Allan, "Evidence for optically induced heating of the GLAS/ICESAT doubler crystal," in *Proc. IEEE LEOS Ann. Meeting*, 2008, vol. 1–9, pp. 216–217.
- [69] D. J. Wingham, C. R. Francis, S. Baker, C. Bouzinac, D. Brockley, R. Cullen, P. De Chateau-Thierry, S. W. Laxon, U. Mallow, C. Mavrocordatos, L. Phalippou, G. Ratier, L. Rey, F. Rostan, P. Viau, and D. W. Wallis, "CryoSat: A mission to determine the fluctuations in Earth's land and marine ice fields," *Adv. Space Res.*, vol. 37, no. 4, pp. 841–871, 2006.
- [70] J. D. Spinhirne, S. P. Palm, and W. D. Hart, "Antarctica cloud cover for October 2003 from GLAS satellite lidar profiling," *Geophys. Res. Lett.*, vol. 32, no. 22, 2005b.
- [71] J. J. Degnan, "Photon-counting multikilohertz microlaser altimeters for airborne and spaceborne topographic measurements," *J. Geodyn.*, vol. 34, no. 3–4, pp. 503–549, 2002.

ABOUT THE AUTHORS

Waleed Abdalati, photograph and biography not available at the time of publication.

H. Jay Zwally, photograph and biography not available at the time of publication.

Robert Bindshadler, photograph and biography not available at the time of publication.

Bea Csatho, photograph and biography not available at the time of publication.

Sinead Louise Farrell, photograph and biography not available at the time of publication.

Helen Amanda Fricker, photograph and biography not available at the time of publication.

David Harding, photograph and biography not available at the time of publication.

Ronald Kwok, photograph and biography not available at the time of publication.

Michael Lefsky, photograph and biography not available at the time of publication.

Thorsten Markus, photograph and biography not available at the time of publication.

Alexander Marshak, photograph and biography not available at the time of publication.

Thomas Neumann, photograph and biography not available at the time of publication.

Stephen Palm, photograph and biography not available at the time of publication.

Bob Schutz, photograph and biography not available at the time of publication.

Ben Smith, photograph and biography not available at the time of publication.

James Spinhirne, photograph and biography not available at the time of publication.

Charles Webb, photograph and biography not available at the time of publication.